Published in final edited form as:
Mol Reprod Dev. 2010 September ; 77(9): 759–772. doi:10.1002/mrd.21217.

Acidic hyaluronidase activity is present in mouse sperm and is reduced in the absence of SPAM1: Evidence for a Role for Hyaluronidase 3 in mouse and human sperm

Kristen L. Reese[2], **Rolands G. Aravindan**[2], **Genevieve S. Griffiths**[2], **Minghai Shao**[2], **Yipei Wang**[2], **Deni S. Galileo**[2], **Vasantha Atmuri**[3], **Barbara L. Triggs-Raine**[3], and **Patricia A. Martin-DeLeon**[2,1]

[2]Department of Biological Sciences, Univ. of Delaware, Newark, DE 19716

[3]Department of Biochemistry and Medical Genetics, University of Manitoba, Winnipeg, MB R3E OW3

Abstract

The molecular mechanisms underlying sperm penetration of the physical barriers surrounding the oocyte have not been completely delineated. Although neutral-active or "reproductive" hyaluronidases (hyases), exemplified by Sperm Adhesion Molecule 1 (SPAM1), are thought to be responsible for hyaluronan digestion in the egg vestments and for sperm-zona binding, their roles in mouse sperm have been recently questioned. Here we report that acidic "somatic" Hyaluronidase 3 (HYAL3) exists in two isoforms in human (~47 kDa, ~55 kDa) and mouse (~44, ~47kDa) sperm where it resides on the plasma membrane over the head and midpiece. Mouse isoforms are differentially distributed in the soluble (SAP), membrane (MBP), and acrosome-reacted (AR) fraction where they are most abundant. Comparisons of zymography of *Hyal3* null and wild-type (WT) AR and MBP fractions show significant HYAL3 activity at pH 3 and 4, and less at 7. At pH 4, a second acid-active hyase band at ~57 kDa is present in the AR fraction. HYAL3 activity was confirmed using immunoprecipitated HYAL3 and spectrophotometry. In total proteins, hyase activity was higher at pH 6 than at 4 where *Spam1* nulls had significantly ($P<0.01$) diminished activity, indicating that murine SPAM1 has acidic activity. Although fully fertile, *Hyal3* null sperm showed delayed cumulus penetration and reduced acrosomal exocytosis. HYAL3, similar to SPAM1 with which it shares 74.6% structural similarity, exists in epididymal tissue/fluid from which it is acquired by caudal mouse sperm *in vitro*. Our results indicate for the first time the concerted activity of both neutral- and acid-active hyaluronidases in sperm.

Keywords

sperm penetration; fertilization; oocyte cumulus complex; ubiquitous or somatic hyaluronidases; sperm-zona binding

INTRODUCTION

The crucial cell adhesion events that are essential for fertilization commence when the sperm bind to the specialized extracellular matrix (ECM) of the oocyte, the zona pellucida (ZP). Yet the mechanism(s) involved have not been fully elucidated. Mammalian hyaluronidases (hyases), a highly conserved family of 6 enzymes, catalyze the breakdown of

[1]Address correspondence to: Patricia A. Martin-DeLeon, Department of Biological Sciences University of Delaware, Newark, DE 19716, Tel. 302-831-2249; Fax. 302-831-2281; pdeleon@udel.edu.

hyaluronic acid (HA) in the ECM (Kreil, 1995; Stern, 2003), and sperm hyases are thought to be involved in ZP-binding. (Myles and Primakoff, 1997; Cherr et al., 2001; Morin et al., 2010). In addition to sperm-egg binding, these multifunctional proteins play a role in the penetration of the cumulus (Myles and Primakoff, 1997; Cherr et al., 2001) and the induction of the acrosome reaction (Vandevoort et al., 1997; Sabeur et al., 1998; Cherr et al., 1999).

Five (3 neutral-active and 2 acid-active) of the 6 hyases are abundantly expressed in the testis (Csoka et al., 1999; Shuttleworth et al., 2002). However only the 3 neutral-active ones, exemplified by Sperm adhesion molecule 1 (SPAM1), are considered to be sperm hyases (Kim et al., 2005; Miller et al., 2007). These neutral-active hyases (HYALP1, SPAM1, HYAL5) which are called “reproductive hyases” are encoded by closely-linked genes (*Hyalp1*, *SPAM1*/*Spam1*, and *Hyal5*) in a cluster on mouse and human chromosome 6A2/7q31 (Csoka et al., 1999; Kim et al., 2005). They are membrane and/or soluble glycosyl phosphatidylinositol-(GPI)-linked proteins and are also expressed in the epididymis (Deng et al., 2000; Evans et al. 2004; Martin-DeLeon, 2006) where SPAM1 has been shown to be acquired on the sperm surface during sperm maturation (Deng et al., 1999; Chen et al., 2006).

Interestingly, these sperm enzymes appear to show functional redundancy as mice lacking either of the two major hyase genes, *Spam1* or *Hyal5*, are fully fertile (Baba et al., 2002; Kimura et al., 2009). Additionally, recent data indicate that both murine SPAM1 and HYAL5 may not play a major role in sperm-ZP binding, as previously envisioned (Kim et al., 2005). Thus the existence of unknown sperm hyase(s) has been proposed in mice (Kimura et al., 2009). It is therefore possible that acid-active hyase(s) expressed in the testis (Csoka et al., 1999; Shuttleworth et al., 2002) may be present, and functionally active, in murine sperm.

Additionally, in mice SPAM1 hyase activity profile has not been fully characterized as in other species where a bimodal activity over a broad pH range of 4.5 to 8.0 for humans (Cherr et al., 2001) and bovine (Oettl et al., 2003) has been recorded. In rats and guinea pigs there is a pH range of 3.6 to 8.6 (Seaton et al., 2000), while in macaques have both acidic (pH 4.0) and neutral (≥pH 7.0) activity have been reported (Cherr et al., 1996). In murine sperm where HYAL5 (55 kDa) and SPAM1 (52 kDa) are active at pH 7.0, Kim et al. (2005) have shown that overall activity decreases slightly at pH 6.0 below which there is no activity for SPAM1 and that below pH 5.0 hyase activity is totally absent. This implies that murine SPAM1 has a narrower hyase activity range than SPAM1 in human, bovine, rat, guinea pig and macaque, and therefore may not be an ideal model for SPAM1.

To address these discrepancies in mice and to increase our understanding of hyases in general, we used available well-characterized mouse mutants in which either *Spam1* (Baba et al., 2002) or *Hyal3* (Atmuri et al., 2008) is deleted, to determine: 1) if the absence of acid hyase activity in mouse sperm could be confirmed, 2) if HYAL3 which belongs to the “somatic” subgroup of hyases, and which is abundantly expressed in the testis, is an unidentified sperm hyase that fulfills the prediction that there are unknown sperm hyases (Kimura et al., 2009); and if so, 3) the characteristics of HYAL3 expression and its involvement in sperm function. Our data show the presence of HYAL3 in human and mouse sperm where it contributes to hyase activity at pH 3, 4 and 7 as well as to cumulus penetration and the induction of the acrosome reaction.

RESULTS

In Silico Analysis

In silico analyses revealed protein characteristics of HYAL3 similar to known functional domains of reproductive hyases, specifically SPAM1. A hydropathy plot analysis of the mouse HYAL3 was generated using the Kyte-Doolittle algorithm and indicates an alternating hydrophilic and hydrophobic pattern with three predicted *N*-linked glycosylation sites corresponding to amino acid positions 69, 216, and 349. Additionally, two epidermal growth factor domains, characteristic of membrane-bound or secreted proteins were identified using Protein families (Pfam) database. Although a consensus glycosyl phosphatidyl-inositol (GPI) anchor site could not be predicted with both Pfam and a second tool, PredGPI (which could also not predict one for SPAM1 which is known to have one), the a Fasciclin domain (Fas1) commonly found in GPI-linked proteins was identified in HYAL3 between amino acid residues 82 and 100. This identified domain is 84.6% similar to the Fas1 domain in GPI-linked HYAL5, suggesting that HYAL3 may also be GPI-linked.

Overall, HYAL3 and SPAM1 proteins are 38.7% identical at the amino acid level, with substantially higher levels of similarity within functional domains. For the functional domains there is an average of 58% similarity. ClustalW alignment of HYAL3 to SPAM1, HYALP1, and HYAL5 shows high similarity in identified functional domains (Supplemental data, Fig. 1). Within the hyase domain there is an increased similarity of HYAL3 to SPAM1, as seen for neutral hyase activity (47%), HA binding (76%), and acidic hyase activity (76.5%). Such increased levels of similarity along HYAL3 and SPAM1 amino acid sequences suggest important physiochemical and functional properties of the proteins for their conserved domains. Importantly, the 30 amino acid hyase activity domain in human hyases (Lokeshwar et al., 2002) has 100% sequence identity to its murine ortholog, as recognized through ClustalW alignment (data not shown).

HYAL3 is expressed in human and mouse sperm

Western blots of total (unfractionated) murine sperm proteins revealed that HYAL3 is present as a single dimer band of ~44 to 47 kDa (Fig 1A). The band was also seen at a lower intensity in the testis where fainter higher MW bands were also seen. Pre-absorption of the antibody with the peptide eliminated the bands from both the sperm and the testis (data not shown) and revealed the specificity of the antibody. To further confirm our results and the specificity of the antibody and unequivocally identify the presence of HYAL3 in sperm, HYAL3 was immunoprecipitated from protein extracts obtained from caput, corpus, and caudal mouse sperm. Western blotting of the immunoprecipitated proteins showed a single ~44–47 kDa band in all three sperm samples (Fig. 1C). In human sperm proteins there were two major bands, one at ~47 kDa and a more prominent one at~55 kDa (Fig. 1A).

When mouse sperm proteins were fractionated after the acrosome reaction, HYAL3 was found to be distributed in all fractions in varying amounts of the two isoforms (Fig. 1B). It was most abundant in AR (acrosome-reacted) sperm fraction with the ~47 kDa band being far more prominent. While both bands were found in the MBP fraction, the ~44 kDa isoform was more abundant and it was the only form seen in the SAP fraction (Fig. 1B). The results indicate that HYAL3 exists in sperm in two isoforms (possibly reflecting different states of glycosylation). The MWs are consistent with 412/417 amino acids in the respective mouse and human protein backbones and potential glycosylation at several sites.

Immunocytochemistry (ICC), using complementary approaches of immunodetection [scanning and transmission electron microcopy (SEM and TEM, Fig. 2B, C,)] and fluorescence (Fig 2E), showed HYAL3 to be present on the plasma membrane of mouse sperm in moderate amounts. This confirmed its presence in the MBP fraction (Fig. 1B).

HYAL3 was localized over the acrosome, as well as on the midpiece of the tail (Fig. 2E) in cells that were not permeabilized. All control samples, treated with rabbit IgG as the primary antibody (Fig.2A, D), showed no labeling.

Murine sperm proteins have acidic hyase activity to which SPAM1 and HYAL3 contribute

Since qRT-PCR revealed that testicular *Hyal3* transcripts are less abundant than those of *Spam1* (data not shown), we reasoned that this might also be the case for HYAL3 compared to SPAM1. Thus to observe any possible enzymatic effect of HYAL3 we loaded 10 μg proteins for hyaluronic acid substrate gel electrophoresis (HASGE) and incubated the gels for 36–48 hr. While this allows the detection of low-activity hyases, it also leads to the coalescence of co-migrated individual hyase bands (due to the closeness of the MWs of the proteins) into a cumulative band. HASGE analysis was performed on total sperm proteins from WT, *Spam1*−/− (null), and *Hyal3*−/− (null) mice and zymography revealed hyase activity at pH 4 and 6, with cumulative hyase activity bands at~45–57 kDa (Fig. 3A). This MW range is consistent with the presence of activity of HYAL5 (55 kDa), SPAM1 (52 kDa) and HYAL3 (44–47 kDa). Activity was lower at pH 4, as indicated by the decreased band intensities and the increased width of the inter-lane spaces which were obliterated at pH 6 (Fig. 3A). While at both pH 6 and 4 the relative lengths of the activity bands were significantly ($P<0.01$) shorter and the widths significantly ($P<0.05$) greater for *Spam1* null compared to WT (Fig. 3B,C), at pH 4 the band areas and densities were significantly ($P<0.01$) smaller than WT (Fig. 3D,F). Our results indicate for the first time that murine sperm not only have hyase activity at pH 4, but that SPAM1 contributes to this activity which is reduced in *Spam1* nulls.

On the other hand, the band areas were not reduced in *Hyal3* nulls, but surprisingly tended to increase at both pH 4 and 6 where the increase was significant ($P<0.05$) (Fig. 3D). This increase in band area for *Hyal3* nulls was accompanied by a significant ($P<0.01$) increase in band width and perimeter (Fig. 3C,E). The latter was not seen for *Spam1* nulls. Overall, for both *Spam1* and *Hyal3* null proteins, the respective absence of SPAM1 and HYAL3 changed the configuration of the bands which appeared more rectangular than squared. The shorter vertical axes of the rectangular null bands are expected from the absence of a hyase in the complement, as shown by Coomassie blue staining (Supplemental Fig. 2). With the full complement of hyases, WT activity bands have a square configuration in contrast to the rectangular appearance in nulls (Fig. 3A).

Fractionated proteins were studied in *Hyal3* null and WT sperm for hyase activity in primarily the AR fraction, where HYAL3 is most abundant. At pH 3 and 4 hyase activity is greater in the AR and SAP fractions compared to the MBP fraction of WT proteins (Fig. 4A, B, C). At pH 4, hyase activity from *Hyal3* null proteins is markedly reduced in the AR fraction, as reflected by a significant decrease ($P<0.005$) in relative band density compared to that of WT (Fig. 4A). The decrease resulted from the absence of a ~44–47 kDa region of the activity band in *Hyal3* nulls (see arrows in Fig. 4A). However, there was no effect on the MBP fraction at pH 4. At pH 7 differences were seen for both the MBP and AR fractions of the mutant and WT, with the AR fraction showing a greater decrease in the relative density in *Hyal3* nulls (Fig. 4A).

At pH 3, where no activity is seen for WT MBP and where WT AR and SAP fractions showed bands that appeared as dimers, the relative decrease in density of the AR fraction for *Hyal3* nulls is ~50% based on the Hsc-70 Western blot loading control (Fig.4B). Since more proteins were actually loaded in the *Hyal3* null sample, the ~50% decrease is a conservative estimate. Thus murine sperm have acidic hyase activity at both pH 3 and 4 to which HYAL3, which also has neutral activity, is a major contributor. Interestingly at pH 4, when 5 μg instead of 10 μg of WT proteins were loaded, a distinct additional ~56–57 kDa band is

seen for the AR fraction and the MBP fraction is missing the ~44–47 kDa band (arrowed) (Fig. 5C). The extra ~57 kDa band appears more prominent in *Hyal3* null samples (data not shown) and suggests that a hyase with a MW higher than that of SPAM1 and HYAL5, is also active at pH 4.

Finally, we used a colorimetric assay and spectrophotometry to confirm the presence of acid-active hyases in murine sperm. Activity in total proteins was present at pH 3, 4, 6 and 7 where it was highest (Fig. 4D). To confirm the role of HYAL3 in sperm hyase activity, an aliquot of the immunoprecipitated HYAL3 from caudal sperm shown in Fig. 1C was analyzed, via the colorimetric assay using rabbit IgG immunoprecipitated sperm proteins as a control. The precipitated HYAL3 protein revealed hyase activity at pH 7.0 and 4.0, with the latter being higher (Fig. 5), directly confirming the findings from the *Hyal3* null proteins in the HASGE assays (Fig. 4A). Immunoprecilitated HYAL3 activity appeared to be similar or greater than that of total proteins (Fig. 5) likely due to the large number of proteins present in the latter.

Functional Activity of HYAL3 in sperm

Cumulus penetration assays were performed to test the impact of the neutral hyase activity of HYAL3. A total of 391 similar-sized oocyte-cumulus complexes (OCC's) were examined in four groups for cumulus penetration as previously described (Chen et al., 2006). Oocytes in Groups 1 (n=130) and 2 (n=92) were incubated with WT sperm treated with rabbit IgG and HYAL3 antibody, respectively; while in Groups 3 (n=73) and 4 (n=96) *Hyal3* null sperm were treated with rabbit IgG and SPAM1 antiserum, respectively. In previous studies no significant difference was observed between sperm incubated with and without rabbit IgG under the conditions used in this study (Chen et al., 2006). Antibody inhibition of HYAL3 on WT sperm was shown to retard cumulus penetration through all four stages, particularly at Stage 2 (Fig. 6A, compare G1 and G2). Chi-squared analysis of the difference in numbers (%) of Stage 4 oocytes seen after WT sperm were treated with IgG or HYAL3 Ab is highly significant ($P < 0.0001$) at 180 and 320 min (Fig. 6B).

Hyal3 null sperm in the presence of rabbit IgG (G3) showed a delay, predominantly at Stage 1, compared to WT sperm identically treated (G1). This delay (Fig 6A) led to a significant decrease in the percentage of Stage 4 oocytes compared to those penetrated by WT sperm identically treated in G1 after 180 ($P< 0.0018$) and 320 min ($P<0.001$) (Fig. 6B). When *Hyal3* null sperm were treated with SPAM1 antiserum prior to introduction to the OOCs (G4), making them essentially “double null” sperm, the lag seen for Stage 1 OOCs for null sperm treated with the IgG (G3) compared to WT (G1) was significantly enhanced ($P=0.027$; Fig.6C). Surprisingly, there was no significant difference in the numbers of oocytes reaching Stage 4 at 180 and 320 min ($P=0.43$; $P=1$) compared to the numbers from those treated with IgG (Fig. 6B, G3 and 4). This finding suggests that in *Hyal3* null sperm SPAM1 contributes only a modest proportion to the overall neutral sperm hyase activity [required for penetration of the cumulus Myles and Primakoff 1997)], although WT sperm were not studied after treatment with SPAM1 antiserum.

To further test the functionality of HYAL3 on the sperm surface, AR was induced by the synergistic action of progesterone (PG) and HA. As expected from our previous study (Morales et al., 2004), there was a significant increase ($P<0.01$) in the number of AR sperm after treatment with HA and PG (Fig. 7). While the addition of rabbit IgG or the HYAL3 Ab alone had no significant ($P>0.05$) effect, the addition of the latter along with HA and PG resulted in a significant reduction ($P<0.01$) in the percentages of AR sperm (36% versus 25.7%). These results suggest that HYAL3 is similar to SPAM1 in that the HA-binding domain that it contains is functional (Morales et al., 2004).

Epididymal expression of HYAL3 and its acquisition by caudal mouse sperm

Because SPAM1, HYALP1, and HYAL5, are expressed in the epididymis (Deng et al., 2000; Zhang and Martin-DeLeon 2001, 2003; Evans et al., 2004; Zhang et al. 2005) where SPAM1 has been shown to be acquired by sperm (Deng et al., 1999; Chen et al., 2006), epididymal tissues and epididymal luminal fluid (ELF) (combined from all three regions), were examined for the presence of HYAL3. HYAL3 was immunoprecipitated from tissue lysates and the ELF, and the immunoprecipitate Western blotted. In both ELF and epididymal tissues Western showed the ~47 kDa HYAL3 band (Fig. 1C,D), identical to that seen in sperm (Fig.1A–C). To confirm that the protein was of epididymal origin we performed RT-PCR for *Hyal3*, and transcripts were present in all three regions of the epididymis (Fig. 1E). While the lower MW band seen for the ELF (Fig. 1C) may be due to protein degradation, the source of the higher band is unknown, but is reminiscent of that seen for caput epididymal SPAM1 (Deng et al., 2000). When caudal mouse sperm were incubated in both unfractionated and fractionated ELF, flow cytometry revealed that HYAL3 can be acquired on the sperm plasma membrane *in vitro* from both the pellet (epididymosomes) and the supernatant (soluble) which was more efficient in delivery of the protein (Fig. 8).

DISCUSSION

Testicular and Epididymal Expression of HYAL3

In silico analyses showed a high degree of amino acid identity in both the HA binding and acidic hyase domains for HYAL3 and SPAM1 which is considered the sperm hyase (Stern, 2003). The identities were 76% and 76.5% respectively, while the neutral hyase domain showed 47.2%. The latter is characteristic only of reproductive hyases (Cherr et al., 2001) and suggests that HYAL3, like SPAM1, has bimodal hyase activity.

The finding of HYAL3 in the testis, using Western, is consistent with previous reports of abundant expression of testicular *Hyal3* transcripts (Csoka et al., 1999; Shuttleworth et al., 2002). Using complementary approaches with HYAL3 antibodies that were previously validated (Hemming et al., 2008) and found in this study to be specific for HYAL3 via pre-absorption with the immunogen, our findings are the first to report the presence of HYAL3 in sperm. Western analysis showed the HYAL3 band to be more intense in sperm than in the testis. This might be so for two reasons: 1) the variety of different testicular cell types, the majority of which might not express HYAL3 and 2) the possibility that sperm HYAL3 is augmented by epididymal HYAL3. ICC revealed that in murine sperm HYAL3 is distributed on the plasma membrane over the head and tail's midpiece, similar to that of SPAM1 (Deng et 1999; Morales et al., 2004). Localization on the head was confirmed by both SEM and TEM. HYAL3's MW of ~44–47 kDa is within the 45–56 kDa range reported for multiple forms resulting from mouse *Hyal3* expression in baby hamster kidney (BHK) cells *in vitro* (Hemming et al., 2008). The mouse sperm isoforms and the ~47–55 kDa human HYAL3 likely represent different glycosylated states, as predicted from the *in silico* analysis and shown in *in vitro* expression (Hemming et al., 2008). At ~44–47 kDa, HYAL3 is the smallest murine sperm hyase, since SPAM1, HYAL5, and HYALP1 have MWs that are ≥ 50 kDa (Miller et al., 2007; Kim et al., 2005; Deng et al., 1999).

Hyal3 transcripts were shown to be present in all three regions of the epididymis and HYAL3 was detected in the epididymis and secreted in the epididymal fluid, similar to *Spam1* (Deng et al., 1999, Zhang and martin- DeLeon, 2003)). Importantly, HYAL3 was acquired *in vitro* on the caudal sperm surface from the ELF in a manner identical to that in which SPAM1 is acquired: the insoluble fraction was more efficient in transferring the protein (Griffiths et al., 2008a,b). Our findings suggest that HYAL3 is acquired *in vivo*

during sperm maturation in the epididymis and that the amount of the protein on the sperm surface may be dependent on the length of time that the sperm are stored in the cauda (Deng et al., 1999). Thus lower amounts of HYAL3 on the sperm surface may be due to shorter storage periods, as implicated for SPAM1 (Martin-DeLeon, 2006).

SPAM1 and HYAL3 contribute to acid hyase activity in mouse sperm

Our finding of HYAL3 in sperm brings the number of sperm hyases to 4 (3 neutral-active and 1 acid-active), and thus is in conflict with a previous report indicating that there are only two murine sperm hyases (Kim et al., 2005). It also fulfills the prediction made by Kimura et al. (2009) that there are unknown hyases, and indicates that hyase activity is a polygenic or quantitative trait in murine sperm. Our study shows for the first time that hyase activity occurs at pH 3 and 4 in mouse sperm, and does not support the report indicating the absence of activity below pH 5 (Kim et al., 2005). The discrepancy between that study and the present, both of which show hyase activity to be highest at pH 7, may lie in the difference in the amount of proteins assayed and the length of the digestion time, The study by Kim et al. (2005) used only 3 μg protein samples, while our studies were performed with 5–10 μg and increased digestion time, both of which would increase the detection of hyases with low activity.

Both HYAL3 and SPAM1 were shown to contribute to acid-active hyase activity in murine sperm. The involvement of SPAM1 was detectable in assays of total proteins, using WT and the well-characterized *Spam1* null mutant (Baba et al., 2002). In considering hyase activity as a quantitative trait, we assessed the relative hyase cumulative band area and density using total sperm proteins and showed them to be significantly decreased for *Spam1* nulls (compared to WT) at pH 4, but not at 6. This strongly indicates that murine SPAM1 has hyase activity at pH 4, a conclusion that calls into question earlier findings showing that the 52 kDa SPAM1 murine hyase band is missing at pH 5 (Kim et al., 2005; Fig. 4). Thus murine SPAM1 which has an acid-active domain is similar to human and bovine SPAM1 which both show bimodal activity on a broad pH range of 4.5 to 8.0 (Cherr et al., 2001; Oettl et al., 2003), and therefore the mouse is an appropriate model for studies of sperm SPAM1.

At pH 6, *Spam1* null proteins showed a significant increase in relative band density and band width, suggesting that there is an upregulation of more neutral hyase(s) in the absence of SPAM1. Evidence for upregulation of sperm hyase in *Spam1* nulls was suggested earlier (Miller et al., 2007) and is also apparent in zymographs published by Kim et al. (2005, Fig. 3) although the authors did not comment on this. Potential hyase(s) that would be involved in upregulation are neutral-active HYAL5 or HYALP1 and this may explain the normal fertility of *Spam1* nulls (Baba et al., 2002).

Although for total proteins *Hyal3* nulls shared with *Spam1* nulls a significant decrease in hyase band length and an increase in band width (Fig. 3B,C), the decrease in band area and density at pH 4 in *Spam1* nulls, relative to WT, were not shared. However the involvement of HYAL3 in both acidic and neutral hyase activity was evident when HYAL3 in subcellular compartments, as well as immunoprecipitated HYAL3, was analyzed. At pH 4 and 3, HA substrate gel electrophoresis (HASGE) showed significant reductions in the hyase bands from *Hyal3* null proteins in the compartment with the majority of HYAL3, the AR fraction. The membrane fraction (MBP) from these nulls also showed a decrease in hyase activity at pH 7, although smaller, consistent with the presence of HYAL3 in moderate amounts in this fraction as detected by Western analysis and immunocytochemistry. This difference in the degree of involvement of HYAL3 in hyase activity at pH 4 and 7 was confirmed when immunoprecipitated HYAL3 was analyzed in a direct approach (Fig. 5). Since human HYAL3 is acid-active *in vitro* with measurable activity at pH 4.2 (Lokeshwar et al., 2002), it

is not surprising that murine HYAL3, with 100% sequence identity to humans, has activity at pH 3 and 4.

The ability for HASGE to conclusively detect the contribution of HYAL3 to hyase activity at pH 4 in *Hyal3* nulls in the AR fraction, but not in total protein, may result from its abundance in the former and the upregulation of existing hyase(s) in the other sperm compartments. It should also be noted that the ~57 kDa hyase band seen at pH 4.0 was more prominent in *Hyal3* nulls in the AR fraction, compared to WT (data not shown), and further suggests upregulation in the nulls of a hitherto unknown sperm hyase which is likely to be HYAL2. The probable involvement of HYAL2 as a sperm hyase is also suggested from the dimer hyase band detected at pH 3.0 and its 50% reduction in *Hyal3* nulls (Fig. 4B). Western analysis confirmed the presence of the 57 kDa HYAL2 in sperm (data not shown). The normal fertility of *Hyal3* nulls (Atmuri et al., 2008) may be explained by upregulation of hyase family member(s), as evidenced by the significant increase in hyase band width (Fig 3A, C) compared to WT.

Thus it is possible that in somatic tissues an upregulation of hyases in *Hyal3* nulls may explain the inability to detect a role for HYAL3 in HA degradation (Atmuri et al., 2008). It is also possible that HYAL3 may not play a major role in HA degradation in somatic tissues (Hemming et al., 2008; Harada and Takahashi, 2007), due to the modest amounts that are present, unlike in the testis where the transcripts are abundant (Coska et al., 1999; Shuttleworth et al., 2002) and may result in the abundance of the protein and ease of detection of its activity in sperm. Further, its activity may be dependent on the presence of molecules not found in somatic tissues, similar to the dependence of HYAL2 activity on the co-expression of CD44 in HEK 293 cells (Harada and Takahashi, 2007).

Roles of HYAL3 in Sperm Function

HYAL3 was shown to play a role in *in vitro* cumulus penetration which occurs at neutral pH (Lin et al., 1994; Cherr et al., 2001). Also the presence of HYAL3 in the ELF and its acquisition on the sperm plasma membrane *in vitro* is consistent with its involvement in cumulus penetration and it being GPI-linked (Chen et al., 2006; Griffiths et al., 2008a, b). There was a marked delay in the progression of oocytes from Stages 1 and 2 for *Hyal3* null sperm, corresponding to the reduction of hyase activity for *Hyal3* null MBP fraction at pH 7.0. The delay was supported by a similar finding for WT sperm that were HYAL3 antibody-inhibited. Both delays resulted in significantly lower numbers of oocytes reaching Stage 4 at 180 and 320 min. Thus the normal fertility of *Hyal3* nulls (Atmuri et al., 2008) is probably due to the redundant neutral hyase activity of HYAL5 or SPAM1 (Kim et al. 2005), and/or HYALP1 (Miller et al., 2007), and their likely upregulation, as mentioned earlier. Note that a marked delay in cumulus penetration was seen for *Spam1* null sperm *in vitro*, yet these mice are fully fertile (Baba et al., 2002) similar to *Hyal3* nulls.

Interestingly *Hyal3* null sperm that were treated with SPAM1 antibody to generate a “double null” phenotype, despite showing an enhanced delay in entering Stage 2, did not differ in the number of oocytes reaching Stage 4. It appears that SPAM1 may contribute only modestly to the overall murine neutral hyase activity, as has been reported by Kim et al. (2005). However, there is the possibility that in *Hyal3* null mice this modest contribution of SPAM1 may have resulted from an apparent upregulation of another hyase(s) leading to a concomitant proportionately lower SPAM1 level. Thus our finding of the involvement HYAL3 in cumulus penetration, along with the earlier demonstration that murine HYALP1 has neutral hyase activity (Miller et al., 2007) support the hypothesis that cumulus penetration is a polygenic (quantitative) trait in mice. Our findings also support the earlier suggestion that there may be crosstalk between hyases (Miller et al., 2007). The crosstalk may occur among hyases in the same cluster, since *Spam1* null protein exhibited

significantly lower hyase band density than WT at pH 4, but not at pH 6 (Fig. 5F). In this regard it should be noted that in cultured cells it was reported that overexpression of HYAL3 appears to augment the activity of HYAL1 (Hemming et al., 2008), implicating crosstalk among more closely related family members.

The presence of HYAL3 on the acrosome, along with its 76% amino acid similarity with SPAM1 in the HA binding domain of the protein predicted from *in silico* studies, suggests a role for HYAL3 in the acrosome reaction signaling pathway via the HA-binding domain (Sabeur et al., 1998; Morales et al., 2004). Experimental studies provided evidence, as there was a significant reduction of the number of HA-enhanced progesterone-induced acrosome reactions after addition of HYAL3 Ab, as compared to controls treated with rabbit IgG.

In addition to a role in cumulus penetration and the acrosome reaction induced physiologically, it is likely that HYAL3 may play a role in penetrating the ZP based on a) its predominant acidic activity and b) its abundance in the AR fraction and hence on acrosome-reacted sperm. Acidic hyase activity has been shown to be required for penetration of the ZP (Sabeur et al., 1997; Cherr et al., 2001). It initially hydrolyzes high MW HA to produce intermediate-sized products which can be further hydrolyzed by neutral hyases (Stern, 2003). A major role for both SPAM1 and HYAL5 in penetrating the ZP has been questioned (Kim et al., 2005). It should be noted that unlike HYAL3, neither is present in large quantities on the inner acrosomal membrane (Kim et al., 2005) that becomes exposed to the ZP after the acrosome reaction. This observation strengthens the argument for the involvement of HYAL3 in the penetration of the ZP. But this remains to be demonstrated.

Taken together, the expression of HYAL3 in testis (where the transcripts are most abundant), sperm, and the epididymis, bolsters the argument for its redefinition as a reproductive hyase. Our findings support the notion of polygenic control of important processes in mammalian fertilization, and show that neutral and acidic hyases play roles in sperm function. They show that murine SPAM1 is similar to human and bovine SPAM1 in having neutral as well as acidic activity in sperm. Importantly, they show for the first time that HYAL3 is a murine sperm protein which, like SPAM1, contributes to both neutral and acidic hyase activity, cumulus penetration, and the induction of the acrosome reaction. The detection of HYAL3 in human sperm reveals that it is conserved and underscores an important role for this protein in mammalian male germ cells. It should be noted that since SPAM1 is the only neutral active hyase in human sperm, unlike the mouse where there are three, our findings suggest that HYAL3's role in sperm function is likely to be proportionately increased in humans compared to that in the mouse.

MATERIALS AND METHODS

In Silico analyses

Hyal3 sequences used in all analyses were obtained from GenBank (Accession # NM_178020). Multiple protein sequence alignments of HYAL3 (NP_821139) to those of SPAM1, HYAL5, and HYALP1 translated from cDNAs (GenBank Accession # AK005638, AK017112, and AK016575, respectively) were performed using ClustalW (European Bioinformatics Institute). Physiochemical similarity of residues was indicated by superimposed color-coding. Putative domains for enzymatic activity of SPAM1 (Cherr et al., 2001) shared by other aligned hyases (Zhang et al., 2005) were highlighted and compared to the HYAL3 sequence for percent similarity and identity. Protein family domains were identified in the HYAL3 sequence using Protein families (Pfam) database (Wellcome Trust Sanger Institute, Washington University in St. Louis, MO).

Animals and Reagents

Sexually mature WT C57BL/6 or ICR (Harlan Sprague-Dawley, Indianapolis, IN) mice as well as *Hyal3* and *Spam1* null mice on the ICR background, 9–20 weeks old, were used in all studies. The *Hyal3* null (or KO) mice, fully fertile, contain a neomycin-resistance (neo) expression cassette inserted into exon 2 and have been characterized (Atmuri et al., 2008). They were generated and provided by Dr. Barbara Triggs-Raine (Univ. Manitoba) via Dr. Euridice Carmona at the University of Montreal, Quebec, Canada. *Spam1* null mice were obtained from the laboratory of Dr. Tadashi Baba (University of Tsukuba, Ibaraki, Japan) where they were generated (Baba et al., 2002). Both nulls were genotyped, using PCR, to ensure their identity upon arrival in our laboratory. Studies were approved by the Institutional Animal Care and Use Committee at the University of Delaware and were in agreement with the Guide for the Care and Use of Laboratory Animals published by the National Institute of health (publication 85-23, revised 1985). The use of human sperm was approved by the University of Delaware Human Subject Review Board and informed consent was obtained from the subjects studied. All enzymes and chemicals were purchased from Fisher Scientific Co. (Malvern, PA), Sigma (St. Louis, MO) or Invitrogen (Carlsbad, CA), unless otherwise specified.

HYAL3 Antibodies

An epitope-purified rabbit polyclonal antipeptide mouse HYAL3 antibody (Ab), (Cat No 38-3700).which cross-reacts with human was obtained from Invitrogen/Zymed (Camarillo, CA). It has been previously validated with respect to its specificity for mouse HYAL3 and its cross-reaction with human (Hemming et al., 2008). The immunogen used in generating the Ab is a unique sequence of 14 residues lying between amino acids #130–230. It was used to confirm the specificity of the antibody in our lab following pre-absorption and Western analysis. A rabbit antipeptide SPAM1 antiserum (Deng et al., 2000) was also obtained from Zymed and has been validated (Zhang and Martin-DeLeon., 2001, 2003a,b, Zhang et al., 2004).

Preparation of Total RNAs from Epididymides

Total RNAs from testes, caput, corpus, and cauda epididymides of 3 to 4-month-old mice were extracted using Tri-Reagent (Sigma, Cat. #T-9424) according to the manufacturer's protocol. Prior to extraction of the RNAs epididymal tissues were minced and washed to remove all sperm as previously described (Deng et al., 2000). RNA samples were subjected to phenol/chloroform extraction and ethanol precipitation.

Reverse Transcriptase-Polymerase Chain Reaction

First strand cDNA synthesis from 2 μg of total RNA was performed with a SuperScript Preamplification System (Qiagen) under the conditions recommended by the manufacturer. Control experiments were performed simultaneously without the addition of RT. Half a microliter of each RT product was subjected to PCR amplification using a pair of primers designed from the 3' UTR of the mouse *Hyal3* cDNA: forward nt 1216–1236; 5'-CTTGGAATTCCTTCAGATGCC-3 ' and reverse primer, nt 1533–1554; 5'-GCTGTCCTGGAACTCACTTT-3' (Integrated DNA Technologies, Inc.; Coralville, IA). The PCRs were performed under the following conditions: 94°C for 2 min, followed by 34 cycles of 94°C for 1 min, 56°C for 2 min, and 72°C for 2 min, and a final cycle of 72°C for 10 min, and holding at 4°C. RT-PCR products were resolved on a 1% agarose gel and stained with ethidium bromide. Triplicate experiments were performed.

Preparation of Protein Extracts and Western Blots

Protein extracts were prepared from the testes of 3–4 month old mice, caput, corpus, and caudal sperm, epididymal tissues [processed and washed to remove sperm as described (Deng et al., 2000)], epididymal fluid [collected as described (Zhang and Martin-DeLeon, 2003)], and and sperm from two fertile men, by manually homogenizing the tissues and cells (using a mortar and pestle) in a solubilization buffer [62.5 mM Tris-HCl, 10% glycerol, 1% SDS, 1 mM phenylmethyl-sulphonyl fluoride (PMSF)] at pH 6.8 and 4°C. The suspensions were centrifuged at 10,000 × g for 10 min at 4°C, and the protein-containing supernatant collected. Protein concentration was determined, using a biocinchoninic acid (BCA) assay kit (Pierce, Rockford, IL). Samples were exposed to reducing conditions [99°C for 4 min in the presence of 100 mM dithiothreitol (DTT)] and processed according to standard protocols (Sambrook and Russell, 2001). Western blotting was performed with the Western Breeze Chemiluminescent Immunodetection Kit (Invitrogen, Carlsbad, CA) according to the manufacturer's protocol. Membranes were probed with the rabbit polyclonal HYAL3 Ab, using AP-conjugated anti-rabbit IgG as the secondary Ab. Heat shock cognate protein 70 (Hsc 70) is abundantly expressed house-keeping protein in sperm and was detected with the primary Ab, as a loading control for proteins assayed for hyase activity.

Sperm Protein Fractionation

Fresh sperm (5×10^7) were collected from minced cauda epididymides of 3–4 month-old males in PBS and washed by centrifugation at 500 × *g* for 15 min. Proteins from these acrosome intact (AI) sperm were extracted with 20 mM Tris-HCl, pH 7.4 containing 0.15 M NaCl, 1% Triton X-100, and 1 mM PMSF. After solubilization on ice for 6 h the sperm suspension was centrifuged at 13,000 × *g* and the proteins recovered in the supernatant. Sperm were acrosome-reacted (AR) as previously described (Deng et al., 1999) after exposure to 5 μg/ml calcium ionophore A23187 at 37°C for 1 h. The suspension was then subjected to centrifugation at 500 × *g* for 15 min to collect AR sperm in the pellet from which proteins were extracted as described above. The supernatant was ultracentrifuged at 100,000 × *g* for 90 min and the supernatant provided soluble proteins (SAP), similar to that described (Kim et al., 2005). The precipitate was washed with PBS and the proteins extracted at 4°C for 6 h in PBS with 1% Triton X-100, 1mM EDTA, 1 mM PMSF and centrifuged at 13,000 × *g* for 10 min. The resulting supernatant was the membranous fraction (MBP) released after the acrosome reaction. The protein concentrations of all samples were determined with the BCA assay kit (Pierce).

Immunoprecipitation of HYAL3 and characterization of its bioactivity

Two aliquots of wild-type mouse epididymal luminal fluid (ELF), epididymal tissue lysate, and sperm lysate each containing 25 μg (ELF), 300 μg (epididymal tissue) or 125 μg (sperm) of total proteins were incubated with either rabbit IgG or rabbit anti-HYAL3 polyclonal antibody (1:500) overnight at 4° C with shaking. At the end of incubation, the HYAL3-antibody complex was precipitated for 1h at RT using Protein G magnetic beads (Millipore, MA) and eluted with 0.2 M glycine (pH 2.5). The eluted proteins were subsequently resolved by 10% SDS-PAGE under reducing conditions, transferred onto nitrocellulose membrane and Western blotted using HYAL3 antibody as per standard protocols. One aliquot was used for hyase activity assays as described below.

Localization of HYAL3 on Sperm using Indirect Immunodetection

The recovery procedure of caudal mouse sperm and the immunocytochemistry (ICC) protocol were as described in Miller et al. (2007), with the exception that the primary HYAL3 antibody and IgG control were used at a dilution of 1:50. For immunocytochemistry, the secondary Ab was FITC-conjugated anti-rabbit IgG (Sigma,

1:400) following which slides were washed with PBS, counter-stained with diaminophenyl-indole (DAPI), and examined with fluorescence microscopy using a Zeiss Axioskop.

For immunodetection of HYAL3 by scanning electron microscopy (SEM), sperm samples were fixed in 4% paraformaldehyde and attached to poly-L-lysine coated coverslips. Coverslips with sperm were blocked in 3% BSA in PBS and immunogold labeled using HYAL3 antibody (1:50) followed by 18 nm gold-conjugated secondary antibody (1:20, Jackson ImmunoResearch, West Grove, PA). Coverslips were washed in filtered PBS, post-fixed in 1% glutaraldehyde in PBS, rinsed in ddH_20, dehydrated in a graded series of ethanol, critical point dried and carbon-coated. All backscattered electron SEM images were acquired at 3kV and 50 microAmp current on a Hitachi S-4700 Field Emission Scanning Electron Microscope with an EXB detector setting −150. Negative controls included normal rabbit IgG and exclusion of primary antibody. For immunodetection by transmission electron microscopy (TEM), paraformaldehyde-fixed sperm samples were floated on formvar coated copper or nickel grids (Electron Microscopy Sciences) before blocking, immunostaining and post-fixing, as described above. Grids were then rinsed in ddH_20 and negatively stained with 2% phosphotungstic acid before imaging with a Zeiss CEM 902 for TEM. Negative controls included normal rabbit IgG and exclusion of primary antibody.

HA Substrate Gel Electrophoresis (HASGE)

Hyase activity in sperm proteins was assayed using HASGE as described (Gunterhoner et al., 1992; Deng et al., 2000; Zhang and Martin-DeLeon, 2003b; Zhang et al., 2004). HA (0.15 mg/ml) from bovine vitreous humor was added to 7.5 or 10% SDS-polyacrylamide gels loaded with 5 or 10 μg of non-reduced proteins and run at 15 mA. After electrophoresis, gels were incubated in 3% Triton X-100 in PBS for 2 h at RT, then at 37°C for 36–48 h in sodium acetate, 12.5–100 mM (pH 3–7). To visualize digestion of HA, gels were stained with 0.5% alcian blue in 3% acetic acid for 2 h, and destained in 7% acetic acid until digestion was visible. Gels were counter-stained with 0.25% Coomassie Brilliant Blue G-250 and de-stained with methanol-acetic acid. Three or more trials were performed at each pH. Gels were scanned and the digitized images analyzed for dimensions of hyase activity bands, as well as density, using Scion Image software (Release ß3b) originally developed at NIH (Bethesda, MD). A Student's "*t*" was used to determine significant differences between the means in WT and nulls.

Spectrophotometric Measurement of Hyase Activity

A colorimetric assay based on alcian blue staining of HA was performed to measure the relative hyaluronidase activity at different pH's, using a method similar to that previously described (Pryce-Jones and Lannigan, 1979) and modified by Kim et al. (2005). Briefly, 1–16 μg bovine testis hyaluronidase standards or 8–32 μg sperm protein extract [125 μg was the starting amount for immunoprecipitated HYAL3] were incubated in triplicates in 600 μl reaction mixture containing 12.5, 25, 50, or 100 mM sodium acetate (pH 3.0, 4.0, 6.0, and 7.0 respectively), 50 mM $MgCl_2$ and 60 μg bovine vitreous humor hyaluronic acid at 37 °C for 30 min. At the end of incubation, 600 ul of 0.02% alcian blue solution in water was added to the reaction mixture and immediately mixed and the precipitate removed by centrifugation at 13,000 × g for 5 min. The absorbance of the supernatant, deemed directly proportional to the hyaluronidase activity, was measured at 600 nm (BioPhotometer, Eppendorf). Significant differences in the means of triplicates were subjected to the Student's "*t*" test to determine statistical significance.

In vitro Fertilization for Vestment Penetration Assay

ICR females (8–10 weeks old) were superovulated and cumulus penetration assays performed as described (Chen et al., 2006), except that *Hyal3* null instead of *Spam1* null

sperm were used. Fresh caudal epididymal sperm from both WT (*Hyal3* +/+) males and those lacking functional HYAL3 (*Hyal3* −/−) were capacitated for 45 min in 1 ml human tubal fluid (HTF) under identical conditions. Capacitated sperm (7.5×10^4) were added to treatment dishes containing 0.5 ml HTF and either rabbit IgG, HYAL3 Ab or SPAM1 antiserum (1:5) for 30 min. Eggs were then incubated with sperm and scored at 20 min intervals (total 6 h) for the degree of cumulus penetration. Analysis of penetration through the cumulus oocyte complexes was as described in our lab (Miller at al., 2007; Chen, et al., 2006; Griffiths et al., 2008b). A 2 × 2 Contingency table was used for statistical analysis.

HA-enhanced Progesterone-induced Acrosome Reaction

Induction of acrosome reactions under conditions that are physiologically relevant, was as previously described from our lab (Miller et al., 2007; Morales et al., 2004). Fresh caudal epididymal sperm (2.5×10^5/ reaction) from 3-month-old WT males were placed in Biggers Whitten & Whittingham (BWW) medium for induction of the acrosome reaction. The sperm suspension was incubated with rabbit IgG or HYAL3 antiserum (1:50) for 10 min at RT. Samples treated with HA (100 μg/mL) for 30 min were subsequently treated with progesterone (PG, 3.18 μM) for 5 min at 37°C for 45 min. Sperm were then pellet by centrifugation (500 × *g*, 15 min) and fixed with 4% paraformaldehyde. Slides were prepared, stained with 0.44% Coomassie Brilliant Blue G-250 in 60% methanol-acetic acid, rinsed in ddH_2O and sealed with Permount. They were blindly analyzed microscopically, for the presence or absence of the acrosomal cap in 200 sperm/slide, as previously described (Morales et al., 2004). Fisher's Exact Test was used for statistical analysis.

In vitro Sperm Acquisition of HYAL3 from the ELF as Detected by Flow Cytometry

ELF was collected and fractionated by ultracentrifugation at 120,000 × *g* as described (Zhang and Martin-DeLeon, 2003; Chen et al., 2006; Griffiths et al., 2008a). Protein concentrations were obtained using the BCA kit (Pierce); Caudal sperm ($2.5–5.0 \times 10^5$) were collected from WT ICR mice, incubated at 32°C in unfractionated ELF or the supernatant or pelleted fractions, as previously described (Chen et al., 2006; Griffiths et al., 2008a,b; Griffiths et al., 2009). Incubation in 2% BSA in PBS served as a negative control. After incubation sperm were recovered by centrifugation, washed and subjected to immunodetection using HYAL3 Ab and an FITC-labeled secondary Ab and flow cytometry, as previously described (Griffiths et al., 2008a, b).

Supplementary Material

Refer to Web version on PubMed Central for supplementary material.

Acknowledgments

We are grateful to Dr. Euridice Carmona, at the University of Montreal for her generosity in making the transfer of the *Hyal3* null mice to our facility possible.

The work was supported by Grants # NIH R01 HD38273 and 5P20RR015588 to (P.A.M-D).

REFERENCES

Atmuri V, Martin DC, Hemming R, Gutsol A, Byers S, Sahebjam S, Thliveris JA, Mort JS, Carmona E, Anderson JE, Dakshinamurti S, Triggs-Raine B. Hyaluronidase 3 (HYAL3) knockout mice do not display evidence of hyaluronan accumulation. Matrix Biol. 2008; 27:653–660. [PubMed: 18762256]

Baba D, Kashiwabara S, Honda A, Yamagata K, Wu Q, Ikawa M, Okabe M, Baba T. Mouse sperm lacking cell surface hyaluronidase PH-20 can pass through the layer of cumulus cells and fertilize the egg. J Biol Chem. 2002; 277:30310–30314. [PubMed: 12065596]

Chen H, Griffiths G, Galileo DS, Martin-DeLeon PA. Epididymal SPAM1 is a marker for sperm maturation in the mouse. Biol Reprod. 2006; 74:923–930. [PubMed: 16436526]

Cherr GN, Meyers SA, Yudin AI, VandeVoort CA, Myles DG, Primakoff P, Overstreet JW. The PH-20 protein in Cynomolgus Macaque spermatozoa: Identification of two different forms exhibiting hyaluronidase activity. Dev Biol. 1996; 175:142–153. [PubMed: 8608861]

Cherr GN, Yudin AI, Overstreet JW. The dual functions of GPI-anchored PH-20: hyaluronidase and intracellular signaling. Matrix Biol. 2001; 20:515–525. [PubMed: 11731269]

Cherr GN, Yudin AI, Li MW, Vines CA, Overstreet JW. Hyaluronic acid and the cumulus extracellular matrix induce increases in intracellular calcium in macaque sperm via the plasma membrane protein PH-20. Zygote. 1999; 7:11–222. [PubMed: 10216912]

Csòka AB, Scherer SW, Stern R. Expression analysis of six paralogous human hyaluronidase genes clustered on chromosomes 3p21 and 7q31. Genomics. 1999; 60:356–361. [PubMed: 10493834]

Deng X, Czymmek K, Martin-DeLeon PA. Biochemical maturation of Spam1 (PH-20) during epididymal transit of mouse sperm involves modifications of N-linked oligosaccharides. Mol Reprod Dev. 1999; 52:196–206. [PubMed: 9890751]

Deng X, He Y, Martin-DeLeon PA. Mouse Spam1 (PH-20): evidence for its expression in the epididymis and for a new category of spermatogenic-expressed genes. J Androl. 2000; 21:822–832. [PubMed: 11105908]

Evans EA, Zhang H, Martin-DeLeon PA. SPAM1 (PH-20) protein and mRNA expression in the epididymides of humans and macaques: Utilizing laser microdissection/RT-PCR. Reprod. Biol. Endocrinol. 2003; 1:54. [PubMed: 12932297]

Griffiths GS, Galileo DS, Reese K, Martin-DeLeon PA. Investigating the role of murine epididymosomes and uterosomes in GPI-linked protein transfer to sperm using SPAM1 as a model. Mol Reprod Dev. 2008a; 75:1627–1636. [PubMed: 18384048]

Griffiths GS, Miller KA, Galileo DS, Martin-DeLeon PA. Murine SPAM1 is secreted by the estrous uterus and oviduct in a form that can bind to sperm during capacitation: acquisition enhances hyaluronic acid-binding ability and cumulus dispersal efficiency. Reproduction. 2008b; 135:293–301. [PubMed: 18299422]

Griffiths GS, Galileo DS, Aravindan RG, Martin-DeLeon PA. Clusterin facilitates exchange of glycosyl phosphatidylinositol-linked SPAM1 between reproductive luminal fluids and mouse and human sperm membranes. Biol Reprod. 2009; 81:562–570. [PubMed: 19357365]

Guntenhoner MW, Pogrel MA, Stern R. A substrate-gel assay for hyaluronidase activity. Matrix. 1992; 12:388–396. [PubMed: 1484506]

Harada H, Takahashi M. CD44-dependent intracellular and extracellular catabolism of hyaluronic acid by hyaluronidase-1 and −2. J Biol Chem. 2007; 282:5597–5607. [PubMed: 17170110]

Hemming R, Martin DC, Slominski E, Nagy JI, Halayko AJ, Pind S, Triggs-Raine B. Mouse Hyal3 encodes a 45- to 56-kDa glycoprotein whose overexpression increases hyaluronidase 1 activity in cultured cells. Glycobiology. 2008; 18:280–289. [PubMed: 18234732]

Kim E, Baba D, Kimura M, Yamashita M, Kashiwabara S, Baba T. Identification of a hyaluronidase, Hyal5, involved in penetration of mouse sperm through cumulus mass. Proc Natl Acad Sci U S A. 2005; 102:18028–18033. [PubMed: 16330764]

Kimura M, Kim E, Kang W, Yamashita M, Saigo M, Yamazaki T, Nakanishi T, Kashiwabara SI, Baba T. Functional Roles of Sperm Hyaluronidases, HYAL5 and SPAM1, in Fertilization in Mice. Biol Reprod. 2009; 81:939–947. [PubMed: 19605784]

Kreil G. Hyaluronidases--a group of neglected enzymes. Protein Sci. 1995; 4:1666–1669. [PubMed: 8528065]

Lin Y, Mahan K, Lathrop WF, Myles DG, Primakoff P. A hyaluronidase activity of the sperm plasma membrane protein PH-20 enables sperm to penetrate the cumulus cell layer surrounding the egg. J Cell Biol. 1994; 125:1157–1163. [PubMed: 8195297]

Lokeshwar VB, Schroeder GL, Carey RI, Soloway MS, Iida N. Regulation of hyaluronidase activity by alternative mRNA splicing. J Biol Chem. 2002; 277:33654–33663. [PubMed: 12084718]

Martin-DeLeon PA. Epididymal SPAM1 and its impact on sperm function. Mol Cell Endocrinol. 2006; 250:114–121. [PubMed: 16420970]

Miller KA, Shao M, Martin-DeLeon PA. *Hyalp1* in murine sperm function: evidence for unique and overlapping functions with other reproductive hyaluronidases. J Androl. 2007; 28:67–76. [PubMed: 16928892]

Morales CR, Badran H, El Alfy M, Men H, Zhang H, Martin-DeLeon PA. Cytoplasmic localization during testicular biogenesis of the murine mRNA for Spam1 (PH-20), a protein involved in acrosomal exocytosis. Mol Reprod Dev. 2004; 69:475–482. [PubMed: 15457544]

Morin G, Sullivan R, Laflamme I, Robert C, Leclerc P. SPAM1 isoforms from two tissue origins are differentially localized within ejaculated bull sperm membranes and have different roles during fertilization. Biol Reprod. 2010; 82:271–81. [PubMed: 19812301]

Myles DG, Primakoff P. Why did the sperm cross the cumulus? To get to the oocyte. Functions of the sperm surface proteins PH-20 and fertilin in arriving at, and fusing with, the egg. Biol Reprod. 1997; 56:320–327. [PubMed: 9116127]

Oettl M, Hoechstetter J, Asen I, Bernhardt G, Buschauer A. Comparative characterization of bovine testicular hyaluronidase and a hyaluronate lyase from streptococcus agalactiae in pharmaceutical preparations. Eur J Pharm Sci. 2003; 18:267–277. [PubMed: 12659938]

Pryce-Jones RH, Lannigan NA. Hyaluronidase: a colourimetric assay [proceedings]. J Pharm Pharmacol. 1979; 31(Suppl):92P.

Sabeur K, Cherr GN, Yudin AI, Overstreet JW. Hyaluronic acid enhances induction of the acrosome reaction of human sperm through interaction with the PH-20 protein. Zygote. 1998; 6:103–111. [PubMed: 9770775]

Sabeur K, Cherr GN, Yudin AI, Primakoff P, Li MW, Overstreet JW. The PH-20 protein in human spermatozoa. J Androl. 1997; 18:151–158. [PubMed: 9154509]

Sambrook, J.; Russell, DW. Molecular Cloning: A Laboratory Manual. 3 ed.. Cold Spring Harbor Laboratory Press; Cold Spring Harbor, NY: 2001.

Seaton GJ, Hall L, Jones R. Rat sperm 2B1 glycoprotein (PH-20) contains a C-terminal sequence motif for attachment of a glycosyl phosphatidylinositol anchor. Effects of proteolytic cleavage on hyaluronidase activity. Biol Reprod. 2000; 62:1667–1676. [PubMed: 10819770]

Shuttleworth TL, Wilson MD, Wicklow BA, Wilkins JA, Triggs-Raine BL. Characterization of the murine hyaluronidase gene region reveals complex organization and cotranscription of Hyal1 with downstream genes, Fus2 and Hyal3. J Biol Chem. 2002; 277:23008–23018. [PubMed: 11929860]

Stern R. Devising a pathway for hyaluronan catabolism: are we there yet? Glycobiology. 2003; 13:105R–115R.

Vandevoort CA, Cherr GN, Overstreet JW. Hyaluronic acid enhances the zona pellucida-induced acrosome reaction of macaque sperm. J Androl. 1997; 18:1–5. [PubMed: 9089061]

Zhang H, Martin-DeLeon PA. Mouse epididymal Spam1 (PH-20) is released *in vivo* and *in vitro*, and Spam1 is differentially regulated in testis and epididymis. Biol Reprod. 2001; 65:1586–1593. [PubMed: 11673279]

Zhang H, Martin-DeLeon PA. Mouse epididymal Spam1 (PH-20) is released in the luminal fluid with its lipid anchor. J Androl. 2003a; 24:51–58. [PubMed: 12514083]

Zhang H, Martin-DeLeon PA. Mouse Spam1 (PH-20) is a multifunctional protein: evidence for its expression in the female reproductive tract. Biol Reprod. 2003b; 69:446–454. [PubMed: 12672666]

Zhang H, Morales CR, Badran H, El Alfy M, Martin-DeLeon PA. Spam1 (PH-20) expression in the extratesticular duct and accessory organs of the mouse: a possible role in sperm fluid reabsorption. Biol Reprod. 2004; 71:1101–1107. [PubMed: 15175239]

Zhang H, Shertok S, Miller K, Taylor L, Martin-DeLeon PA. Sperm dysfunction in the Rb(6.16)- and Rb(6.15)-bearing mice revisited: involvement of *Hyalp1* and *Hyal5*. Mol Reprod Dev. 2005; 72:404–410. [PubMed: 16078272]

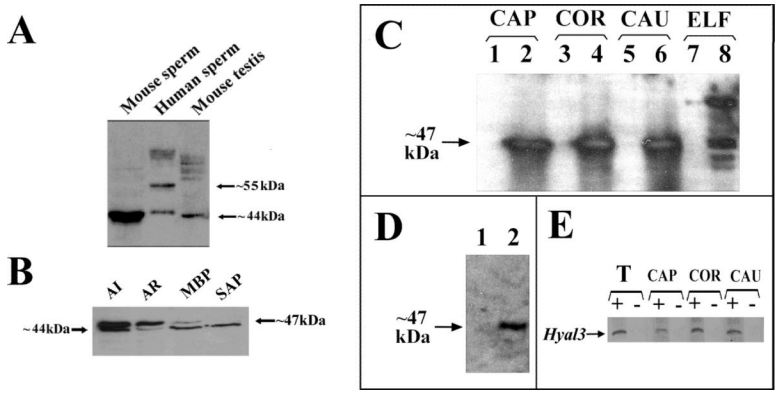

Fig. 1. HYAL3 is conserved in human and mouse sperm, where it is distributed in different subcellular compartments, and is present in the epididymis

A) Western blot shows the ~44–47 kDa HYAL3 in WT mouse sperm and testis proteins (40 μg). Human sperm proteins (40 μg) show two isoforms at ~ 47 and 55 kDa. Pre-absorption of HYAL3 Ab with the immunizing peptide eliminated the bands, indicating the specificity of the antibody (data not shown). **B)** Subcellular localization of HYAL3 is seen in WT mouse proteins (15 μg) from acrosome–intact (AI) sperm and all three fractions following the acrosome reaction: acrosome- reacted (AR), membrane-bound (MBP) and the soluble acrosomal (SAP) fraction. Two isoforms are seen with different proportions in the fractions, except for the SAP which has only the smaller isoform. **C)** Immunoprecipitation unequivocally revealed the presence of HYAL3 in mouse sperm. Non-specific rabbit IgG (lanes 1,3,5,7) and HYAL3 (lanes 2,4,6,8) immunoprecipitated proteins from lysates of wild-type mouse caput (CAP), corpus (COR), and cauda (CAU) sperm and epididymal luminal fluid (ELF) show the 47 kDa band with Western blotting. **D)** Immunoprecipitated epididymal tissue also shows the band (lane 2) with lane 1 being the IgG control. **E)** RT-PCR revealed the presence of *Hyal3* transcripts in all three regions of the epididymis, using the testis, T, as a positive control.

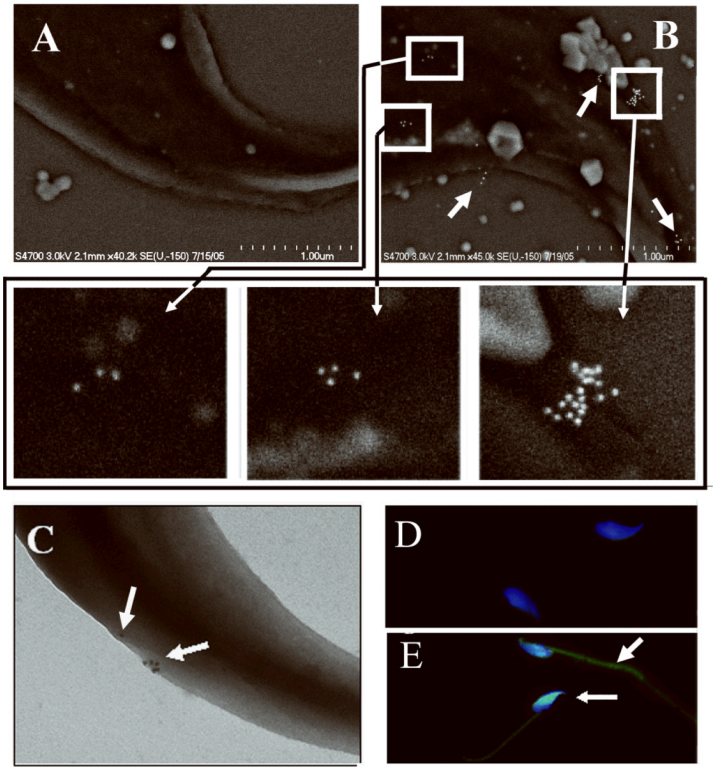

Fig. 2. HYAL3 is immunolocalized on the surface of mouse sperm head and the tail's midpiece

Scanning (**B)** and transmission **(C**) EM images of sperm treated with HYAL3 antibody and the 18 nm immunogold-conjugated secondary Ab show dispersed gold particles (arrowed and box) on the head over the acrosome. The boxed gold particles are enlarged in the middle panel. The control treated similarly, but without the primary antibody, shows no gold particles for both SEM (**A)** and TEM (data not shown) (magnification. × 85,000). [Polygonal structures in A and B are salt crystals]. Immunofluorescent images confirm the localization of HYAL3 over the acrosome, and localize it on the midpiece of the tail as well, with the FITC-conjugated secondary antibody staining green (**E**). The staining has a punctate appearance (which implies movement of the protein) and is absent in the controls (**D**) where rabbit IgG was used as the primary Ab. Both test and controls are counterstained blue with DAPI.

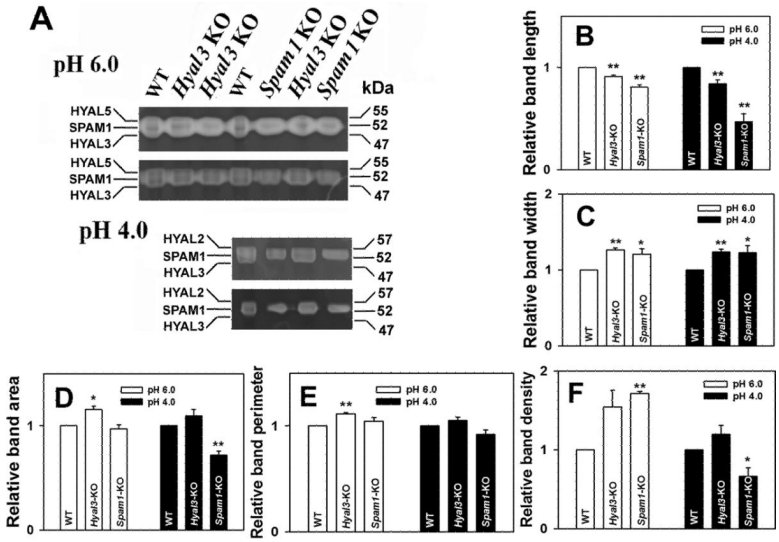

Fig. 3. Murine sperm have hyase activity at pH 4 to which SPAM1 significantly contributes

Representative gel**s** in HA substrate gel electrophoresis (HASGE) assays of total protein (10 μg) show activity at pH 4 is lower than at pH 6, where the inter-lane spaces are obliterated due to HA digestion. The cumulative activities of hyases in total proteins render the configurations of the visualized bands different, depending on the absence of individual hyases. In general the absence of a hyase changes the dimensions of the activity bands. The co-migrated hyase bands from *Spam1* null proteins have a rectangular configuration, compared to WT (square) at both pH 4 and 6 due to the missing protein (Fig. 2, Supplemental data online). A similar, but less attenuated configuration, is seen for *Hyal3* null proteins. **B)** When WT band lengths were normalized to 1, a *`t'* test showed that relative band lengths of hyase activity were significantly shorter for *Hyal3* and *Spam1* nulls (**P<0.001) at pH 6 and 4. **C)** Band widths were significantly greater for *Hyal3* (**P<0.001) and *Spam1* (*P<0.01) nulls, suggesting upregulation of remaining hyase(s). **D–F)** At pH 6 and 4 band area (*P<0.01), perimeter (**P<0.001), and density were generally higher in *Hyal3* nulls than WT. While for *Spam1* nulls they were approximately the same or higher (**P<0.001) at pH 6, they were significantly lower than WT at pH 4 (**P<0.001 in **D**, *P<0.01 in **F**). Thus *Spam1* is an important contributor to hyase activity at pH 4.

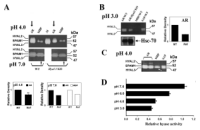

Fig. 4. Substrate gel assays of WT and *Hyal3* null fractionated sperm proteins reveal that HYAL3 in the AR fraction contributes significantly to hyase activity at pH 3 and 4 (where a hyase band at 57 kDa, the MW of HYAL2, is also seen), and lesser at 7

A) *Hyal3* null AR proteins (10 μg) show decreased activity at pH 4 where the relative band densities from 3 independent trials are significantly ($P<0.005$) less than WT (lower panel), due to a missing segment at ~ 44–47 kDa of cumulative activity band (large arrows). No difference is seen for the MBP fraction, indicating that HYAL3 does not contribute to hyase activity of MBP at pH 4 in WT proteins. At pH 7 both the AR and the MBP fractions (small arrows) for *Hyal3* nulls are smaller than WT, as shown by the relative density (lower panel), indicating that both HYAL3 fractions contribute to different degrees to the activity. **B**. Lanes contain 5 μg proteins. At pH 3 no activity is seen for the WT MBP, and the WT AR fraction is twice as dense as that from *Hyal3* null proteins, indicating that HYAL3 contributes ~50% of the hyase activity. The lower panel shows a Western blot of Hsc70, encoded by a housekeeping gene, used as a loading control for AR proteins. In **C** (5 μg WT protein) in the AR fraction, in addition to the co-migrated ~45–55 kDa bands there is a distinct 57 kDa band, more pronounced in the sample on the right. Note here, as in **A**, the absence of a 44–47 kDa band (arrowed) in WT MBP compared to the AR and SAP fractions at pH 4, consistent with physiological requirements *in vivo*. **D**. The colorimetric spectrophotometric assay confirms the presence of acidic hyase activity in murine sperm (WT) proteins and shows it to be pH dependent and positively related.

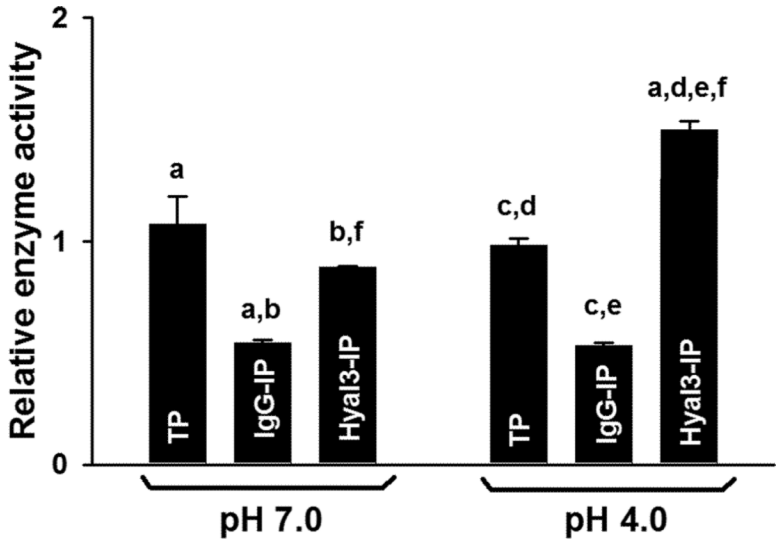

Fig. 5. A Comparison of neutral and acidic HYAL3-specific activities in mouse sperm assayed by colorimetry reveals higher activity at pH 4 than at 7

Hyase activity in HYAL3 immunoprecipitated aliquots was not only detected when compared with IgG immunoprecipitates at pH 7.0 and pH 4.0, but was shown to be significantly greater in the latter. This is consistent with HYAL3 being an acid-active hyase. Bars with similar superscript letters indicate statistically significant differences among groups, using the Student's "*t*" test. Error bars denote SEM. TP = total protein.

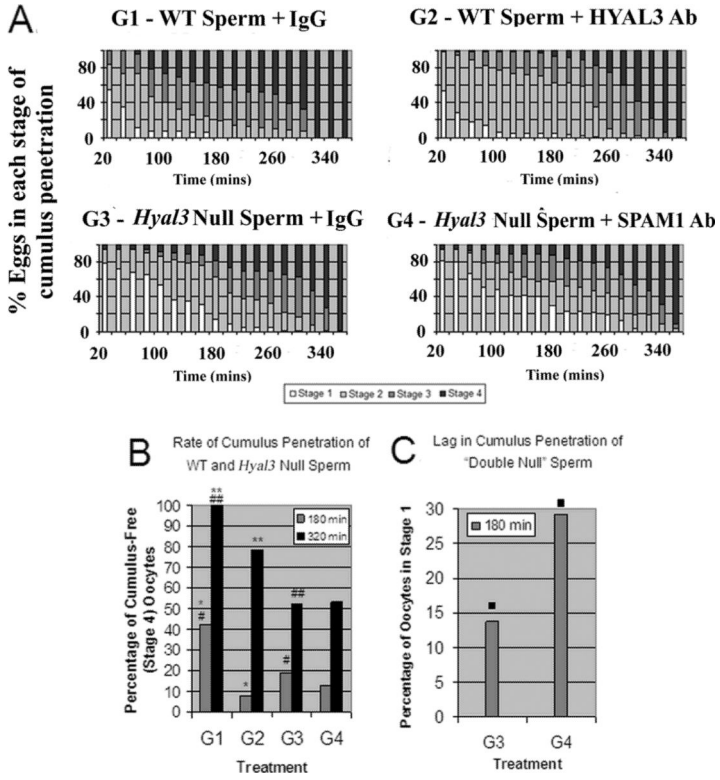

Fig. 6. The rates of cumulus penetration by *Hyal3* null and WT sperm and of WT sperm treated and untreated with HYAL3 antibody are significantly lower for the nulls and treated sperm

Eggs were assessed as being in Stage 1 when surrounded by tightly packed cumulus cells that occlude the oocytes, Stage 2 when oocytes are partially visible with most of the cumulus retained, Stage 3 when most of the cumulus is shed and the zona is visible, and Stage 4 when cumulus-free. **A)** Penetration by WT sperm (Groups 1 and 2) is retarded through all stages, particularly at Stages 1 and 2 when HYAL3 is antibody-inhibited (Group 2). In the presence of rabbit IgG, *Hyal3* null sperm (Group 3) were also retarded compared to WT similarly treated (Group 1). Antibody-inhibition of SPAM1 of *Hyal3* null sperm, "double null" (Group 4), resulted in a more severe lag at Stage 1 than seen in null sperm in IgG. **B)** Penetration of HYAL3 antibody-inhibited WT sperm at 180 and 320 min after incubation was complete in significantly fewer oocytes than those in IgG ($P<0.001$)*, **. Inhibition of *Hyal3* null sperm in IgG compared to WT in IgG also led to significantly fewer cumulus-free eggs ($P< 0.0018$) at $180^{\#}$ and $320^{\#\#}$ min ($P<0.001$). At these times there were no significant differences ($P= 0.43$; $P=1$) in the number of cumulus-free oocytes in Groups 3 and 4. However in **C)** a comparison of % of oocytes incubated with *Hyal3* null and "double null" sperm shows a significantly more severe lag ($P=0.027$)■ for the latter in the entry of oocytes into Stage 2 at 180 min. A 2 × 2 Contingency Table with a $\chi 2$ test was used for all statistical analyses.

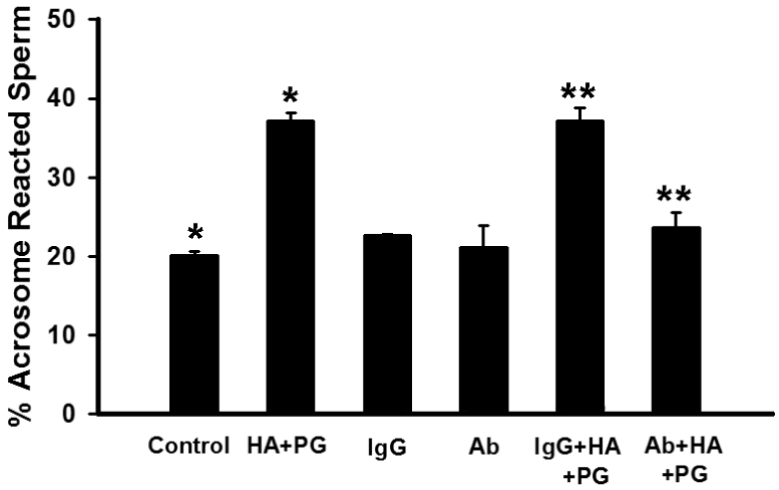

Fig. 7. Results of HA-enhanced progesterone induced acrosome reaction suggest that HYAL3 is involved in the acrosome reaction HA signaling pathway of sperm

The synergistic effects of HA and progesterone (PG) on sperm from WT males (n=3) resulted in a significant increase ($P < 0.01$)* in the number of AR sperm, compared to controls. While the addition of IgG or HYAL3 antibody (Ab) alone resulted in similar numbers of AR sperm as controls, there was a significant decrease ($P<0.01$)** of the enhancement with HA and PG in the presence of HYAL3 antibody inhibition, using Fisher's exact test.

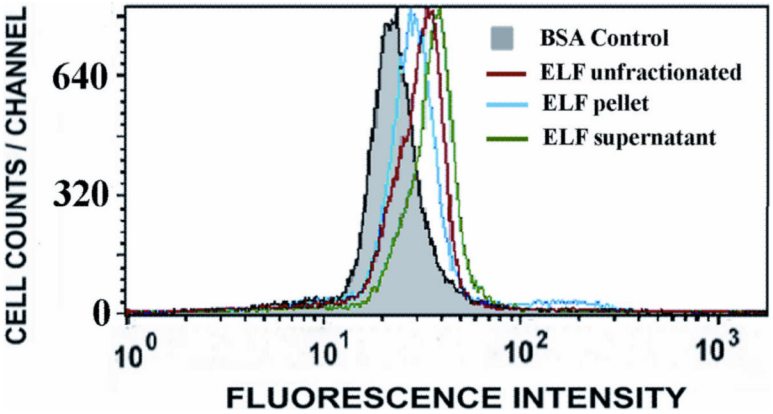

Fig. 8. Flow cytometric analysis of sperm acquisition of HYAL3 from unfractionated and fractionated ELF

HYAL3 is acquired on the sperm surface of WT caudal sperm after incubation in ELF and its fractions (1mg/ml protein) at 32°C for 2 h. Controls were incubated in BSA (gray). Test samples were the unfractionated, pelleted (epididymosomes), and supernatant fractions. In each group 5×10^4 sperm were analyzed. Results, representing 3 trials, indicate a substantial uptake of HYAL3 from ELF.